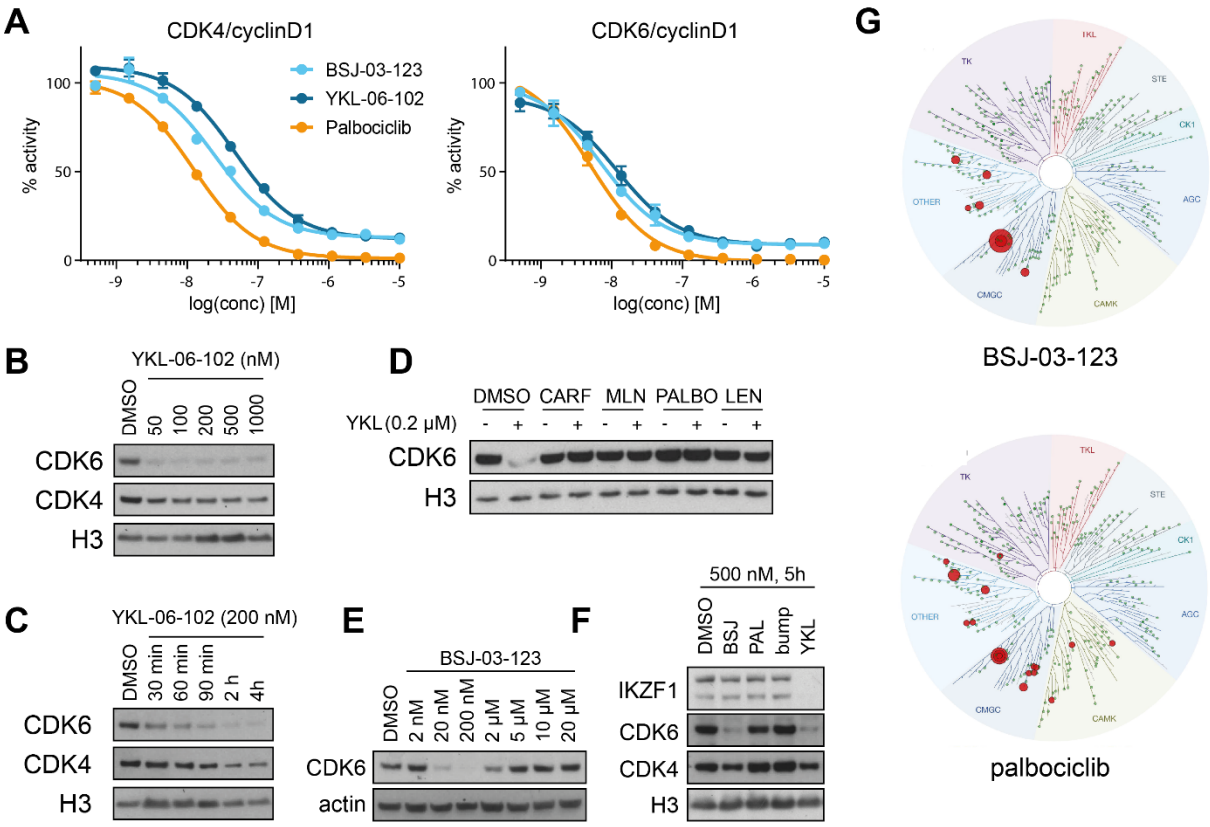

Supplementary Figure 1, related to Figure 1. (A) *In vitro* kinase inhibition assay for palbociclib, YKL-06-102 and BSJ-03-123 on recombinant CDK4/CyclinD1 and CDK6/CyclinD1. **(B)** Immunoblot for CDK4, CDK6 and histone 3 after dose-ranging treatment with YKL-06-102 for 4 hours. **(C)** Immunoblot for CDK4, CDK6 and histone 3 after time-resolved treatment with YKL-06-102 (200 nM). **(D)** Chemical competition experiment. Immunoblot for CDK6 and histone 3 after 1 h pre-treatment with DMSO, 500 nM carfilzomib (proteasome inhibitor, CARF), 1 µM MLN4924 (neddylation inhibitor, MLN), 10 µM palbociclib (PALBO) or 10 µM lenalidomide (LEN), followed by 2 h treatment with DMSO or 200 nM YKL-06-102. **(E)** Immunoblot for CDK6 and actin after extended dose-ranging treatment with BSJ-03-123 for 2 hours. **(F)** Immunoblot for IKZF1, CDK4, CDK6 and histone 3 after prolonged treatment (5h) with 500 nM BSJ-03-123, Palbociclib, YKL-06-102, BSJ-bump or DMSO. **(G)** Comparison of interaction of BSJ-03-123 and palbociclib with 468 human kinases (KINOMEscan). Compounds were tested at 1 µM concentration. Bound kinases are indicated by red circles of size proportional to the percentage of binding to each kinase.

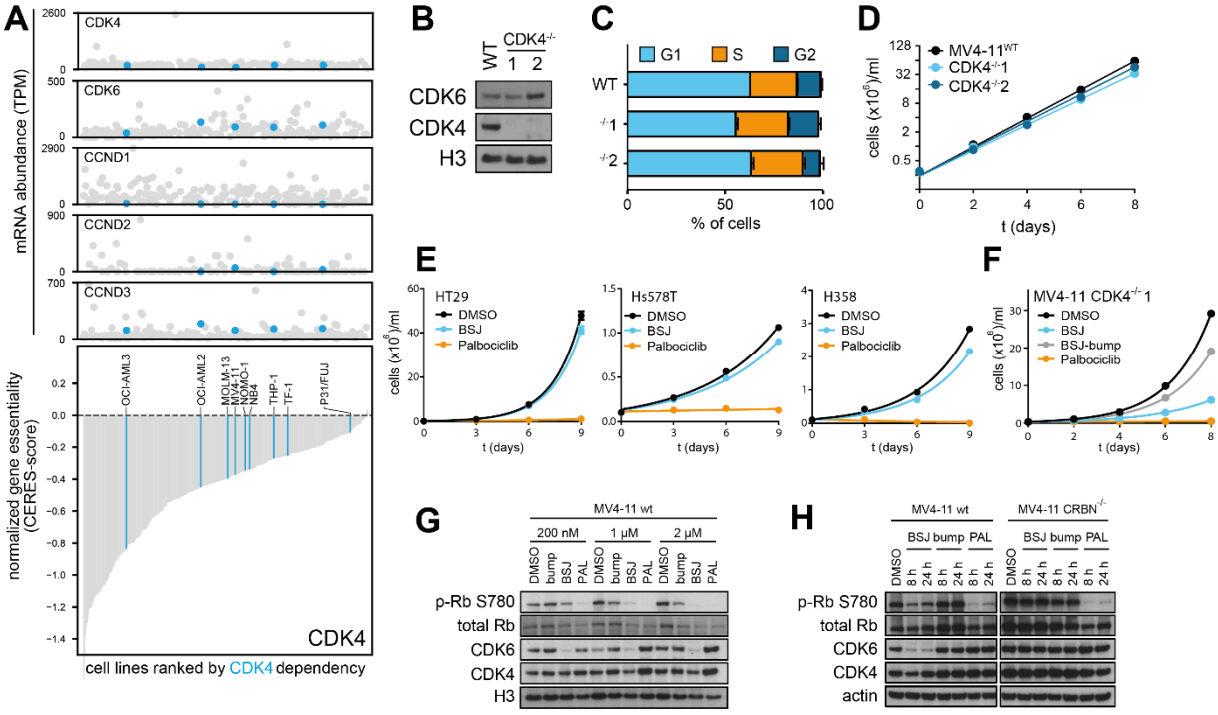

Supplementary Figure 2, related to Figure 3. (A) Bottom: Waterfall plot of 391 cell lines ranked by CKD4 dependency as determined in genome-wide CRISPR/Cas9 screens (Meyers et al., 2017). The CERES essentiality score is normalized for copy number variation of the gene of interest and scaled by setting the median of pan-essential genes to -1. Top: mRNA levels of CDK4, CDK6 and D-type cyclins extracted from RNA sequencing data in cancer cell lines (Klijn et al., 2015). AML cell lines are highlighted in blue. **(B)** Immunoblot for CDK4, CDK6 and histone 3 in MV4-11 wt and two CDK4-deficient clones. **(C)** Cell cycle distribution in *wild-type* and CDK4-deficient MV4-11 as determined by propidium iodide staining **(D)** Growth curves of *wild-type* and CDK4-deficient MV4-11. Cells were counted every 2 days. **(E)** Growth curves of CDK6-independent cell lines HT29, Hs578T and NCI-H358 treated with 200 nM BSJ-03-123, palbociclib or vehicle (DMSO). Cells were counted and re-seeded with drug every 3 days. **(F)** Growth curves of CDK4-deficient MV4-11 treated with 200 nM BSJ-03-123, BSJ-bump, palbociclib or vehicle (DMSO). Cells were counted and treatment refreshed every 2 days. **(G)** Immunoblot for p-Rb S780, total Rb, CDK4, CDK6 and histone 3 after 24 h treatment with BSJ-03-123, palbociclib or BSJ-bump at the indicated concentrations. **(H)** Immunoblot for p-Rb S780, total Rb, CDK4, CDK6 and actin after treatment with 200 nM BSJ-03-123, palbociclib, BSJ-bump or DMSO for the indicated time in *wild-type* or CRBN-deficient MV4-11.

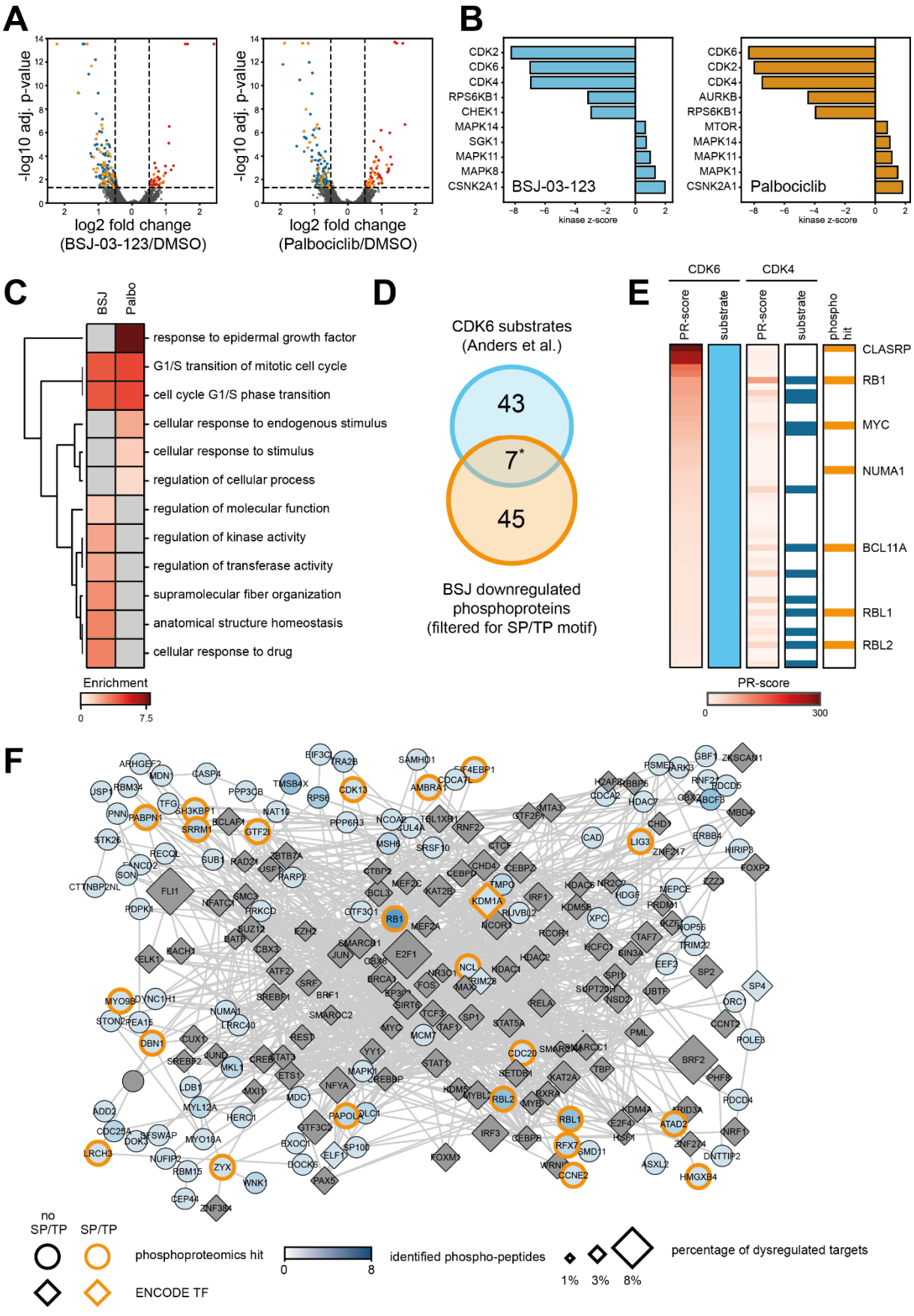

Supplementary Figure 3, related to Figure 4. (A) Global phosphoproteomics. Scatter plots of fold change of peptide phosphorylation relative to DMSO after BSJ-03-123 or palbociclib treatment (200 nM,

2h) versus significance. Downregulated phosphopeptides (log2 FC < -0.5, p-value < 0.05) are highlighted in blue, upregulated phosphopeptides (log2 FC > 0.5, p-value < 0.05) in red. Peptides phosphorylated at a CDK consensus motif SP/TP are highlighted in yellow. **(B)** z-score normalized kinase prediction scores as determined by kinase-substrate enrichment analysis on hits of the global phosphoproteomics experiment. Top 5 significantly enriched and depleted kinases are plotted. **(C)** Clustered heatmap of GO term enrichment analysis of differentially phosphorylated peptides. The color intensities indicate the level of enrichment score of each GO term. **(D)** Intersection of phosphoproteomics data with putative CDK6 targets (Anders et al., 2011). *p = 4.49×10^{-5} (hypergeometric test) **(E)** Relative phosphorylation (PR-) scores for CDK6 and CDK4 of the 50 CDK6 targets from Anders et al. detected in the phosphoproteomics experiment. Downregulated hits from the BSJ-03-123 phosphoproteomics are highlighted in orange. **(F)** Molecular network of palbociclib treatment. Hits identified via global phosphoproteomics were mapped on a protein-protein interaction network and expanded to include first order neighbors limited to ENCODE transcriptional regulators. Node shape distinguishes transcriptional regulators (TR, diamonds) from phosphoproteomics hits (round). Node color represents the number of quantified phosphopeptides. Diamonds are scaled proportional to percentage of dysregulated TR target genes upon treatment. Proteins phosphorylated at CDK consensus motif (SP/TP) are annotated by edge color. Edges represent physical interaction between proteins.

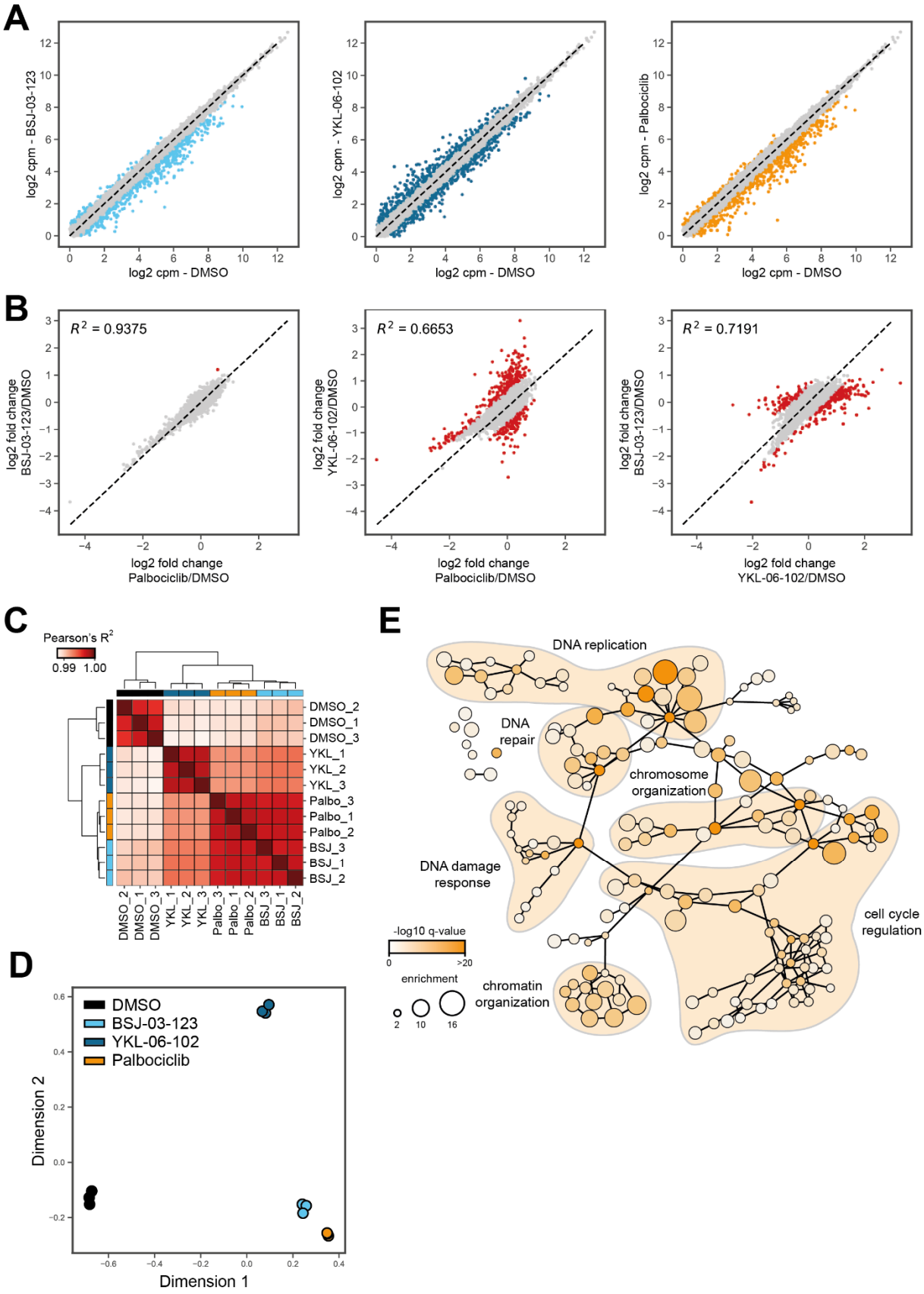

Supplementary Figure 4, related to Figure 4. (A) Scatter plots of expression levels for each gene in MV4-11 treated with BSJ-03-123, YKL-06-102 or palbociclib (200 nM, 6h) compared to DMSO. Significantly differentially expressed genes are highlighted. **(B)** Scatter plots of pairwise comparisons of

gene expression changes upon BSJ-03-123, YKL-06-102 or palbociclib treatment (200 nM, 6h). log2 transformed fold changes relative to DMSO control are plotted for each treatment. Significantly differentially expressed genes are highlighted in red. **(C)** Clustered heat map depicting the Pearson correlation coefficient of pairwise comparisons between technical replicates of the RNA sequencing experiment in MV4-11. **(D)** MDS plot of individual technical replicates of the RNA sequencing experiment in MV4-11. **(E)** Functional network of palbociclib treatment. Nodes represent GO-terms enriched among genes that are differentially expressed upon Palbociclib treatment, scaled by magnitude and color coded by significance of enrichment. Edges represent parent-child relationships of GO-terms.

Supplementary Table 1, related to Figure 1. Biochemical characterization of probes used in this study.

compound	IC50 CDK4-cyclin D1 (nM)	IC50 CDK4-cyclin D3 (nM)	IC50 CDK6-cyclin D1 (nM)	IC50 CDK6-cyclin D3 (nM)	IC50 CRBN (µM)*
Palbociclib	13.7	19.5	6.2	30.7	n.d.
YKL-06-102	74.6	47.8	13.5	305.7	2.2
BSJ-03-123	41.6	31.2	8.7	228.7	2.2
BSJ-bump	19.9	41.1	4.2	95.4	inactive

*lenalidomide 4.62 µM
n.d.=not determinded